



**HAL**  
open science

# Granular modeling of swelling clays: a bottom-up approach

Farid Asadi, Laurent Brochard

► **To cite this version:**

Farid Asadi, Laurent Brochard. Granular modeling of swelling clays: a bottom-up approach. 25ème Congrès Français de Mécanique, Aug 2022, Nantes, France. hal-03994293

**HAL Id: hal-03994293**

**<https://enpc.hal.science/hal-03994293v1>**

Submitted on 17 Feb 2023

**HAL** is a multi-disciplinary open access archive for the deposit and dissemination of scientific research documents, whether they are published or not. The documents may come from teaching and research institutions in France or abroad, or from public or private research centers.

L'archive ouverte pluridisciplinaire **HAL**, est destinée au dépôt et à la diffusion de documents scientifiques de niveau recherche, publiés ou non, émanant des établissements d'enseignement et de recherche français ou étrangers, des laboratoires publics ou privés.

# Granular modeling of swelling clays : a bottom-up approach

F. ASADI<sup>a</sup>, L. BROCHARD<sup>a</sup>

a. Laboratoire Navier (UMR 8205), ENPC, Univ. Gustave Eiffel, CNRS, Marne-la-Vallée, France  
contact: laurent.brochard@enpc.fr

## Résumé :

*A l'échelle sub-micrométrique, la méso-structure de la matrice argileuse et son rôle dans le comportement thermo-hydro-mécanique (THM) restent méconnus car cette échelle est très difficilement accessible à l'imagerie directe. Sur la base d'un nouveau modèle granulaire développé récemment, nous étudions dans cet article l'évolution de la méso-structure sous chargements mécanique et osmotique. Le modèle est une approche purement 'bottom-up' élaborée à partir de résultats de simulations moléculaires, et qui parvient à reproduire quantitativement le comportement THM usuel des argiles. On s'intéresse à quelques ingrédients clés de la méso-structure : le degré d'anisotropie locale, la flexibilité des minéraux argileux, les états d'hydratation. Il apparaît ainsi qu'à forte pression de confinement la méso-structure perd la mémoire de sa structure initiale et les minéraux présentent une flexion significative. La déshydratation, induite par chargement mécanique ou osmotique, est très sensible aux hétérogénéités de contraintes et donc à l'histoire de chargement. Une description des hétérogénéités à l'échelle méso apparaît ainsi indispensable à la compréhension fine du comportement THM des argiles.*

## Abstract :

*At the sub-micrometric scale, the meso-structure of clay matrix and its role in the thermo-hydro-mechanical (THM) behavior remains poorly known because this scale is hardly accessible to direct imaging. Based on a newly developed granular model, we study in this article the evolution of the meso-structure under mechanical and osmotic loadings. The model is a pure bottom-up approach coarse grained from molecular simulation results, which is quantitatively consistent with the usual THM behavior of clays. We focus on a few key features of the meso-structure: the degree of local anisotropy, the flexibility of the clay minerals, and the hydration states. It appears that at high confining pressures the meso-structure loses memory of its initial structure and the minerals exhibit a significant bending. The de-hydration, induced by mechanical or osmotic loading, is highly sensitive to the stress heterogeneities and thus to the loading history. A description of the heterogeneities at the meso-scale thus appears essential to the fine understanding of the THM behavior of clays.*

**Mots clefs / key words : swelling clay, cohesive grains, mesoscale, bottom-up**

# 1 Introduction

Clays are geo-materials containing extremely fine mineral grains with peculiar hydro-mechanical behavior, the most well-known being the drying shrinkage. Indeed, the nanometric mineral layers can adsorb water in the inter-layer, which induces large deformations. Although, the crystalline swelling at the layer scale was identified long ago in the 1950's by XRD, much progress in its fundamental understanding has been made in the last 20 years thanks to the development of molecular simulations. Atomistic modeling offers an unprecedented nanoscale description of the mechanisms of swelling, with quantitative estimates of the mechanical behavior at the scale of a single mineral layer, in particular the coupling with humidity and the thermo-mechanical response [2]. Yet, the up-scaling from the mineral layer to the clay matrix remains a challenge, in particular because the meso-scale (nm to  $\mu\text{m}$ ) is hardly accessible to experimental observation, and the microstructure at this scale can only be inferred indirectly (e.g., from small angle scattering). As an alternative to experiments, granular 'meso-scale' simulations have emerged which aim at taking advantage of the fine understanding obtained at the molecular scale to propose 'coarse-grained' models at larger scales. We recently proposed a meso-scale model for sodium Wyoming montmorillonite [1], designed to investigate specifically the anomalous thermo-hydro-mechanical couplings. In this work, we use this meso-scale model to investigate in detail the mesostructure and its evolution during mechanical and osmotic loadings. In particular, we investigate in this paper the evolution of local anisotropy due to the stacking of clay layers, the deformability of the layers and the changes in hydration states of the layers.

## 2 Method

### 2.1 Coarse grained potential

The proposed meso-scale model is a coarse-graining of the molecular scale, and we summarize hereafter the salient features of the set up of this model (see full details in [1]). The meso-scale clay matrix is modeled in 2D, with chains of particles representing the flexible mineral layers of nanometric thickness (Fig. 1). In such a description, a particle corresponds to a small portion of a hydrated clay layer and water hydration is implicit and accounted for through the inter-layer interactions.

Inter-layer interaction at the nanoscale is peculiar in swelling clays: some inter-layer distances are unstable (non convex energy) and others are (meta-)stable (convex portions), which defines distinct hydration states 'xW' corresponding to the formation of x water layers in the inter-layer space [2]. For instance sodium montmorillonite (Na-Mnt) can be found in the hydrations states 0W (dry state), 1W, 2W and 3W, that correspond to inter-layer distances of  $\sim 9.5 \text{ \AA}$ ,  $\sim 12.5 \text{ \AA}$ ,  $\sim 15.5 \text{ \AA}$ , and  $\sim 18.5 \text{ \AA}$ . At larger distances, this layering effect vanishes and on recovers capillary behavior in the pore, which we refer to as the 'suspension' state. In this work, we limit ourselves to one hydration transition (2W-1W) which is the most important one for Na-Mnt swelling, occurring near 65% of relative humidity at ambient condition. The interaction between particles of neighboring layers is modeled with a simple double well potential with as few parameters as possible (expression in Tab. 1, representation in Fig. 2 left). The overall interaction between two parallel layers involves many particle-particle interactions but the double well nature of the interaction is preserved allowing for an accurate calibration on the disjoining pressure isotherm of Na-Mnt obtained from molecular simulation [2] (Fig. 2 right). The disjoining pressure characterizes the mechanical response orthogonal to the layer only, and one must also address

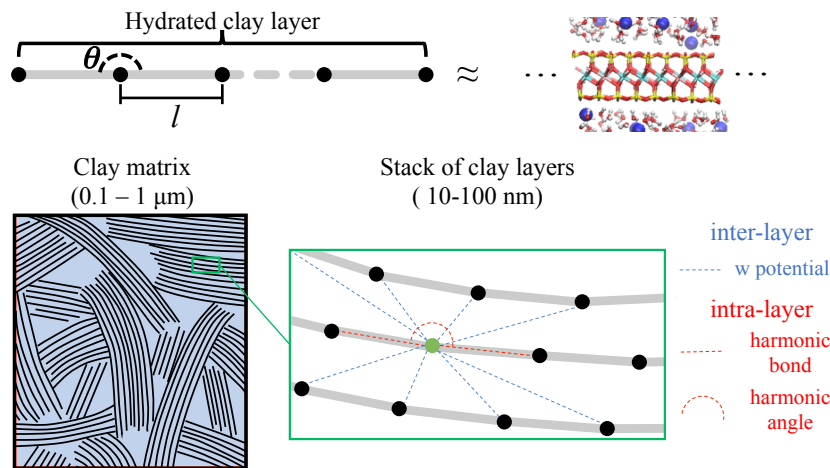


Figure 1: Schematic representation of the 2D granular mesoscale model of clay. Chains of particles represents flexible hydrated clay layers. Intra-layer energy is modeled by nearest neighbors interactions with harmonic bonds and angles. Inter-layer energy is modeled by the double well pair potential ( $w$  potential, see Fig. 2 and Tab. 1) capturing the 1W and 2W hydration states.

Table 1: Interaction potential and calibrated parameters of the meso-scale model

|   |            |           |           |                                     |                 |                         |                |
|---|------------|-----------|-----------|-------------------------------------|-----------------|-------------------------|----------------|
| Intra-layer   |            |           |           |                                     |                 |                         |                |
| $E_{angle}(\theta) = K_{angle}(\theta - \theta_0)^2$  |            |           |           | $E_{bond}(l) = K_{bond}(l - l_0)^2$ |                 |                         |                |
| Inter-layer   |            |           |           |                                     |                 |                         |                |
| $E_{inter-layer}(r) = \int_r^{+\infty} F(u) du$ with $F(r)$ linear by part as described in Fig. 2 |            |           |           |                                     |                 |                         |                |
| $K_2$ (N/m)   | $r_1$ (nm) | $l_0/r_1$ | $K_1/K_2$ | $(r_2 - r_1)/r_1$                   | $F_0/(K_2 r_1)$ | $K_{angle}/(K_2 r_1^2)$ | $K_{bond}/K_2$ |
| 0.06  | 1.28       | 0.25      | 7         | 0.22                                | 0.025283143     | 61                      | 400            |

the shear behavior for a realistic description of the inter-layer interaction. In this respect, the two shear strengths of the 1W and 2W hydration states [4] were also calibrated by adjusting the intra-layer distance between neighboring particles. Since shear strengths ( $\sim 5 - 25$  MPa) are much lower than the compressive barrier ( $\sim 100$  MPa) between hydration states, this calibration results in a inter-layer interaction with small variations in shear relative to the variations in compression. This calibration is critical to guarantee a realistic meso-scale model, in particular with respect to hydration transition and inter-layer sliding/friction. Regarding intra-layer interactions, harmonic bonds and angles involving closest neighbors only were considered (Fig. 1) and the moduli were calibrated to reproduce the elongation and bending stiffnesses of the mineral layer obtained by molecular simulation [5] (Tab. 1).

## 2.2 Mesostructures

Using the coarse-grained model, a 2D assembly of a few tens of thousands of particles corresponds to systems of a few hundreds of nanometers, i.e., the scale of the clay matrix. The arrangement of minerals layers is poorly known at this scale, but mineral layers are often observed in locally stacked configurations, and an important indicator of the microstructure is the number of layers in a stack [6]. A preparation method was proposed [1], which makes it possible to generate meso-structures with desired degree of stacking. This method consists in preparing a highly dilute configuration, and submit it to a constant compression rate while the system evolves according to a brownian dynamics at constant temperature. In this process, it appears that the degree of stacking at the end of the preparation depends directly on the compression rate, offering a simple way to generate meso-structures of controlled degree

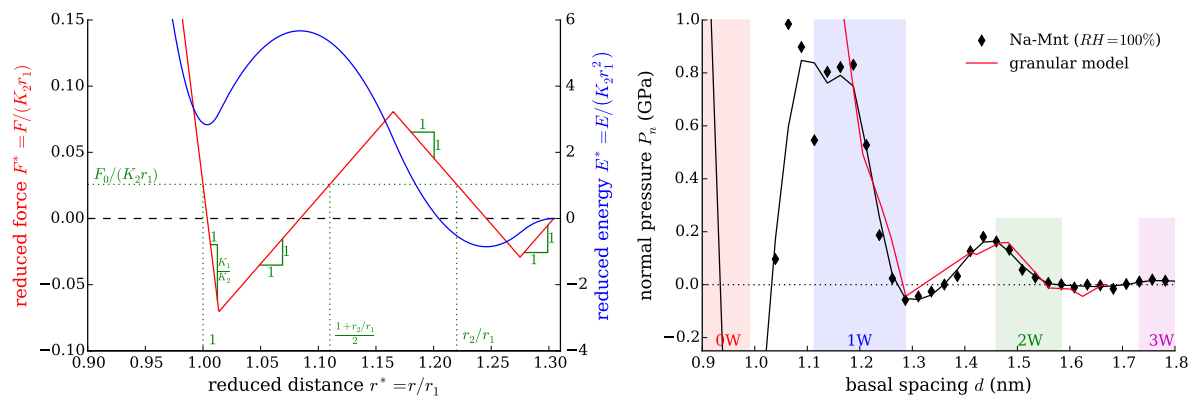


Figure 2: (left) Double well potential (w potential) used to model the inter-layer interactions. (right) Calibration of the potential on the 1W-2W portion of the disjoining pressure isotherm of sodium Wyoming montmorillonite obtained by molecular simulations [2]. The calibration of the 2D model on 3D disjoining pressure assumes a thickness  $l_0$  of 2D system in the third dimension ( $l_0$  is the equilibrium distance between two particles in a chain). The same thickness is then used to extrapolate 2D results in 3D.

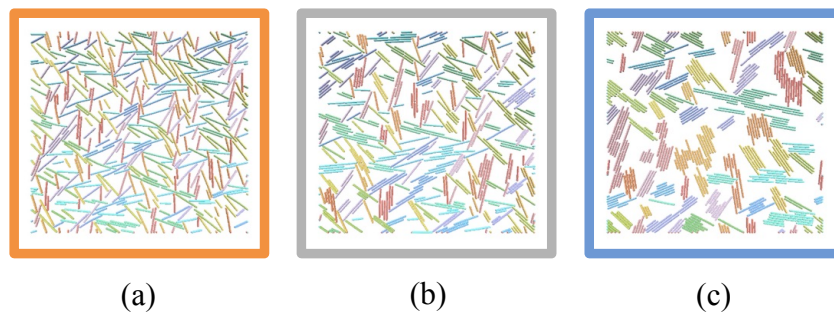


Figure 3: Initial mesostructures generated with different degrees of stacking: little stacking (a), moderate stacking (b), and important stacking (c). The color scale is used to highlight the orientations of the clay layers.

of stacking (see details in [1]). This method was used to generate three meso-structures with different degrees of stacking (Fig. 3), that will serve as initial configuration for all the investigations of this paper. The highest degree of stacking corresponds to  $5.7 \pm 3.3$  layers per stack, which is reasonably consistent with experimental estimations [6]. Yet, high resolution microscopy is mostly sensitive to ordered domains, and one cannot exclude that the clay matrix contains less ordered domains. So we consider the three meso-structures as equally valid initial configurations.

## 2.3 THM loadings

### Mechanical loading: isotropic compression

By construction, the meso-scale model captures the drained behavior of Na-Mnt, since it is calibrated on the mineral layer behavior at constant water activity. The reference case considered is the Na-Mnt at 100% relative humidity, for which the 2W state is energetically favored over the 1W state. As the system is compressed, the most favorable hydration state changes from 2W to 1W, and this hydration transition is associated with a sudden change in the inter-layer distance. For the ideal case of perfectly parallel layers compressed in the direction normal to the layer, hydration transition is expected to occur

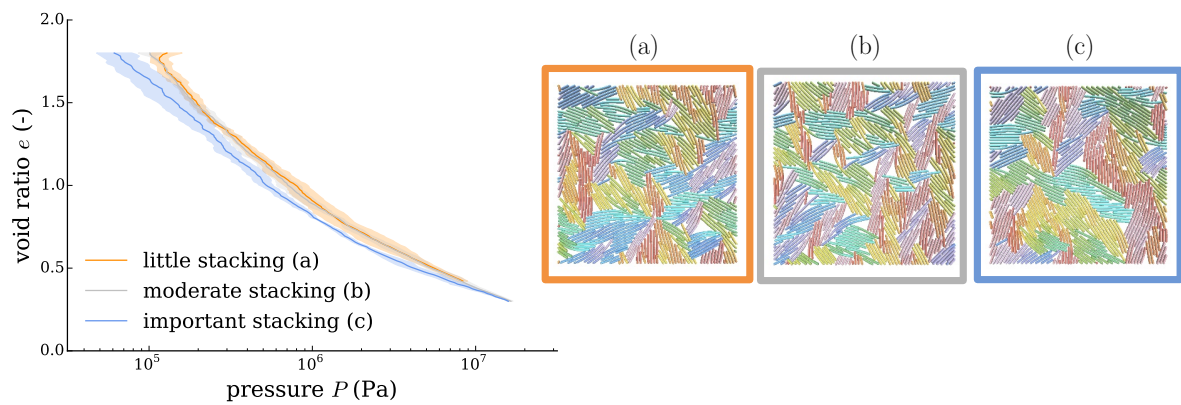


Figure 4: (left) Mechanical response of the three mesostructures of Fig. 3 upon isotropic compression, characterized by the pressure-void ratio curves. (right) Evolution of the three mesostructures at the end of the compression.

at large pressures exceeding 100 MPa. But, for heterogeneous meso-structures with flexible layers, stress concentrations could well induce hydration transitions at much lower pressures. Hereafter, we investigate the mechanical response of the meso-scale model by submitting the three meso-structures to isotropic compression. As before, the systems evolve following a Brownian dynamics while a constant engineering strain rate is applied, but the temperature considered is much smaller (5 orders of magnitude) in order to approach quasi-static conditions. The mechanical response of the material is consistent with usual observations for montmorillonite : the pressure increases exponentially (Fig. 4 left) approaching  $P = 0.8 \text{ MPa}$  at a void ratio  $e = 1$  and with a quite typical compression modulus ( $de/d \log(P) = 0.9 \pm 0.05$ ). Interestingly, the three consolidation curves converge to almost the same curve when approaching 10 MPa, and the associated mesostructures appears very similar based on visual observation (Fig. 4 right).

### Osmotic loading: drying/humidification

Hydration transition can also be triggered by osmotic loading. As relative humidity is decreased, or temperature increased, the most favorable hydration state changes from 2W to 1W, which triggers a shrinkage. Such osmotic loading can be simply modeled by changing the additive constant  $F_0$  of the

inter-layer force (Fig. 2 left). A remarkable value of  $F_0$  is  $F_0^{eq} = \frac{K_1(r_2-r_1)}{\frac{K_1}{K_2}-1} \left( \frac{3\frac{K_1}{K_2}+1}{\sqrt{8\frac{K_1}{K_2}\left(\frac{K_1}{K_2}+1\right)}} - 1 \right)$  for

which the w potential provides equal energies to the 1W and 2W wells. The reference case of Na-Mnt at 100% relative humidity is more favorable to the 2W well (Fig. 2), which corresponds to a higher value of  $F_0$ :  $F_0 = 2.5F_0^{eq}$ . Decreasing  $F_0$  from its reference value to  $-1.0F_0^{eq}$  leads to the opposite situation with respect to the relative energies of the 1W and 2W states (Fig. 5 left). Hereafter, we investigate the osmotic response of the meso-scale model by submitting the meso-structures to variations of  $F_0$  ( $2.5F_0^{eq}$  to  $-1.0F_0^{eq}$ , and back to  $2.5F_0^{eq}$ ) while maintaining constant pressure on the systems with a Berendsen barostat. Again, the quasi-static response is approached by considering a Brownian dynamics at low temperature. Two loading histories are investigated : a normally consolidated system at 1 MPa, and an over-consolidated system at 0.1 MPa (pre-consolidation at 1 MPa). The osmotic cycle induces a

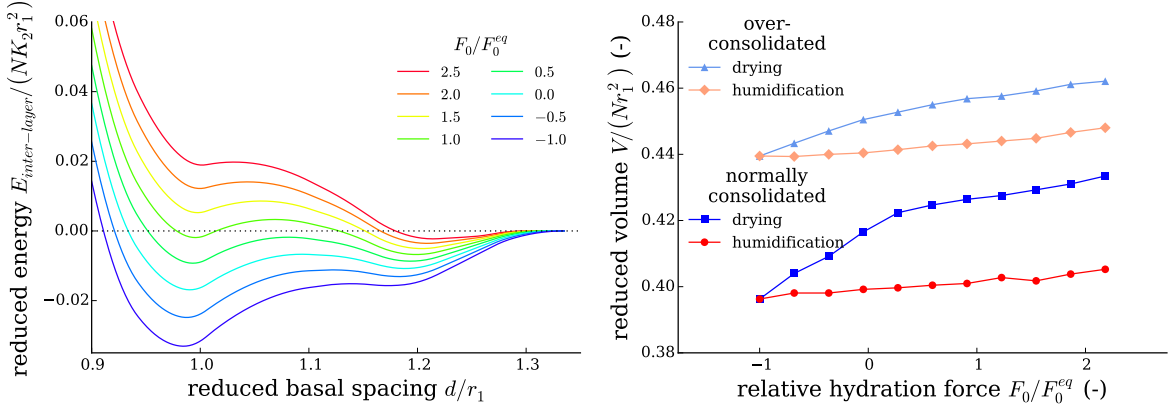


Figure 5: (left) Osmotic loading triggering hydration transition is simulated by changing the value of the reference force  $F_0$  (Fig. 2 left). De-hydration is simulated by varying  $F_0$  from its original value  $2.5F_0^{eq}$  favorable to the 2W state to  $-1.0F_0^{eq}$  favorable to the 1W state. Re-hydration is then simulated by applying the inverse evolution. (right) Volume change of systems during the de-hydration/re-hydration cycle. The permanent shrinkage strongly depends on the consolidation state.

permanent shrinkage that is much more pronounced for the normally consolidated case than for the over-consolidated case (Fig. 5), which recalls experimental observations, e.g., drained heating tests [3].

In this paper, we analyze in detail several aspects of the evolution of the meso-structures during these mechanical and osmotic loadings:

- the local order of the meso-structure by considering the nematic order parameter  $Q$  defined as the positive eigenvalue of the average order two tensor  $\mathbf{Q} = \langle \mathbf{Q}_i \rangle_\Omega$  over a sub-volume  $\Omega$  of the meso-structure, with the per particle tensor defined by :  $(\mathbf{Q}_i)_{kl} = 2u_i^k u_i^l - \delta_{kl}$  for  $(k, l) \in \{x, y\}$  and  $(u_i^x, u_i^y)$  the vector normal to the chain at the position of the particle  $i$  (obtained as average of the normal to the bonds connected to particle  $i$ ). A highly ordered volume  $\Omega$  (perfect stacking) exhibits a nematic order parameter  $Q = 1$ , whereas a perfectly isotropic volume  $\Omega$  is characterized by  $Q = 0$ .
- the importance of layer deformation (bending and elongation quantified by  $E_{angle}$  and  $E_{bond}$ , respectively, in Tab. 1) by considering the relative contribution of intra-layer and inter-layer interactions in the total energy.
- the local hydration states (1W, 2W, suspension) by determining the state of each particle based on an inter-layer distance criterion (see detailed criterion in [1]).

## 3 Results

### 3.1 Isotropic compression

#### Local order and stacking

The local nematic order parameter  $Q$  quantifies the anisotropy in a sub-volume  $\Omega$  of the system. By dividing the system in equal square sub-cells of length  $l = L/n$  ( $L$  system size and  $n$  an integer), we estimate the average nematic order parameter  $Q(l)$  associated to a specific sub-cell size  $l$ . Since the

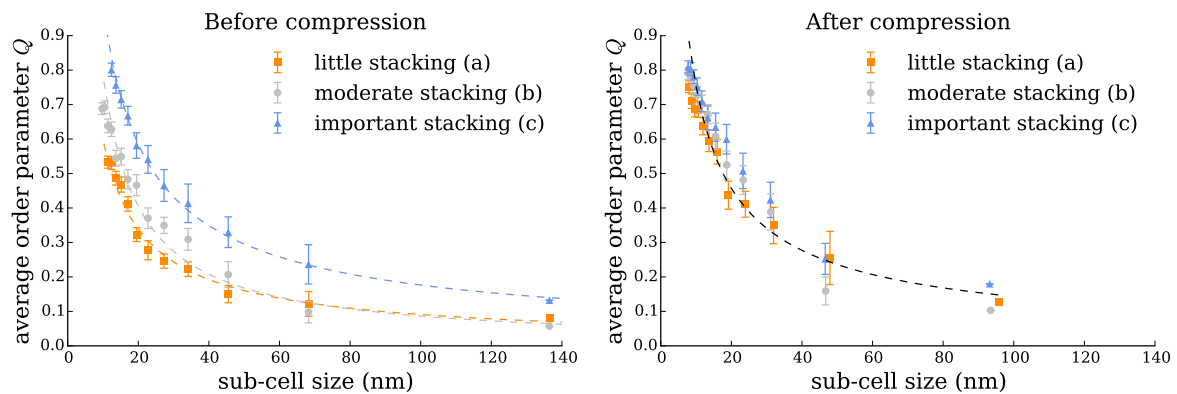


Figure 6: Local nematic order parameter  $Q$  for the three initial meso-structures of Fig. 3 before (left) and after (right) isotropic compression.

three meso-structures are globally isotropic but locally anisotropic (Fig. 3), one expects a nematic order parameter close to 0 for  $l = L$  and approaching 1 for  $l \rightarrow 0$ . This is indeed what is observed for the three initial meso-structures before compression (Fig. 6 left). A clear hierarchy appears because of the difference in the degrees of stacking : the higher the stacking the higher the order parameter  $Q$ . Isotropic compression up to  $\sim 10$  MPa strongly modifies the meso-structures (Fig. 4 right) so that one hardly makes the difference with the naked eye, and the mechanics of the system seems to converge to the same consolidation curve (Fig. 4 left). This suggests that, at high compression, the systems tends to loose memory of the initial configuration. Looking at the nematic order parameter after compression (Fig. 6 right) tends to confirm this analysis: the local order parameter appears very similar for all the three initial configurations. A slight hierarchy is preserved but the differences are very modest.

### Importance of intra-layer bending and elongation

If the deformation of the layers seems negligible for the initial meso-structures before compression, some moderate deformations of the layers appear after compression (Fig. 4 right). Layer bending and stretching are captured by the intra-layer potential made of harmonic angles and bonds, which were calibrated initially to reproduce the bending and elongation moduli of clay minerals estimated by molecular simulations [5]. But this initial calibration led to excessively stiff elastic response [1]. Elastic stiffness appears to be controlled by the combined effect of layer stiffness and layer length [5] and the layer lengths of the three meso-structures (6 to 20 nm) is not representative of actual layers (a few hundred nm). One can unbiased the elastic behavior by reducing the layer stiffness to compensate for the small layer length, so that the resulting elastic behavior becomes representative of actual clays. Doing so, the angle and bond moduli were recalibrated to the values of Tab. 1 [1]. This corrected parameterization is expected to provide a realistic picture of the layer deformation under THM loadings. To quantify the importance of layer deformation, we display in Fig. 7 the evolution of the bond, angle and inter-layer energies during the isotropic compression for the meso-structure (c) of Fig. 3. The energies are reduced with respect to the minimum energy  $E_0 / (NK_2r_1^2) = -0.00677$  corresponding to perfectly parallel undeformed layers in the 2W energy well. Moreover, the inter-layer energy is shifted by  $E_0$  to ensure positive values only. It appears that intra-layer stretching remains almost negligible in comparison with the two other energies ( $< 1.5\%$  of the total energy). However, layer bending contribution is quite significant. More



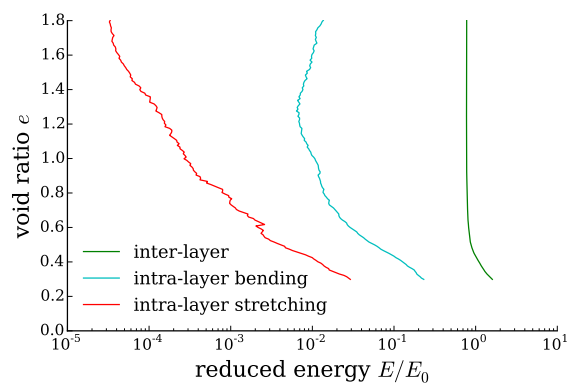


Figure 7: Evolution of the bond, angle and inter-layer energies during isotropic compression for the meso-structure (c) of Fig. 3.

precisely, the bending energy remains modest for void ratios exceeding  $e = 0.8$  (i.e.,  $P < 1$  MPa) with less than 2% of the total energy, but then it increases by one order of magnitude, reaching about 12% of the total energy at the end of the compression. Thus one can distinguish two regimes : 1) at low pressures ( $< 1$  MPa) layers are almost undeformed and can be considered as rigid bodies, 2) at high pressures ( $> 1$  MPa) layers bend significantly and this bending is expected to play an important role in the mechanical response by making the system more compliant than with infinitely rigid layers.

### Hydration transition

One specificity of the mesoscale model is that it captures the hydration states of the clay layers thanks to the double well potential. In the framework of this model we are able to distinguish three hydration states: 1W corresponding to the one water layer state of Na-Mnt usually observed under free stress conditions at relative humidities between 15% and 65%, 2W corresponding to the two water layers state of Na-Mnt usually observed at relative humidities between 65% and 95% and suspension (or  $\infty$ W) corresponding to the full exfoliation in liquid water. For sake of simplicity, the mesoscale model was limited to a single hydration transition (1W-2W), and neglects the 0W dry state (RH below 15%) and the 3W state (RH above 95%). One can easily determine the hydration state of any given particle of the mesoscale model by looking at the inter-particle distances between neighboring layers (see [1]). Thus we are able to follow the detailed evolution of the hydration state during any THM loading. For perfectly parallel layers the 2W-1W hydration transition is expected at very high pressures exceeding 150 MPa (see Fig. 2 right). Yet, stress concentration in heterogeneous meso-structure is likely to promote progressive hydration transitions during compression. We display in Fig. 8 the fraction of the different hydration states in the system and the evolution during the isotropic compression for the meso-structure (a) of Fig. 3. The chart is illustrated with snapshots of the meso-structure where the particles are colored in function of their respective hydration states. At the beginning of compression the system contains about half 2W and half suspension. This initial hydration configuration strongly depends on the degree of stacking: more stacking favors more 2W state over suspension, but in all cases the proportion of 1W remains minor (see [1]). Fig. 8 shows two successive evolutions: 1) at pressures below 3 MPa, the fraction of 1W remains moderate, while most of the suspension states turn into 2W state, 2) at pressures above 3MPa, the fraction of 1W dramatically increases and replaces all the 2W. Although it is expected that hydration

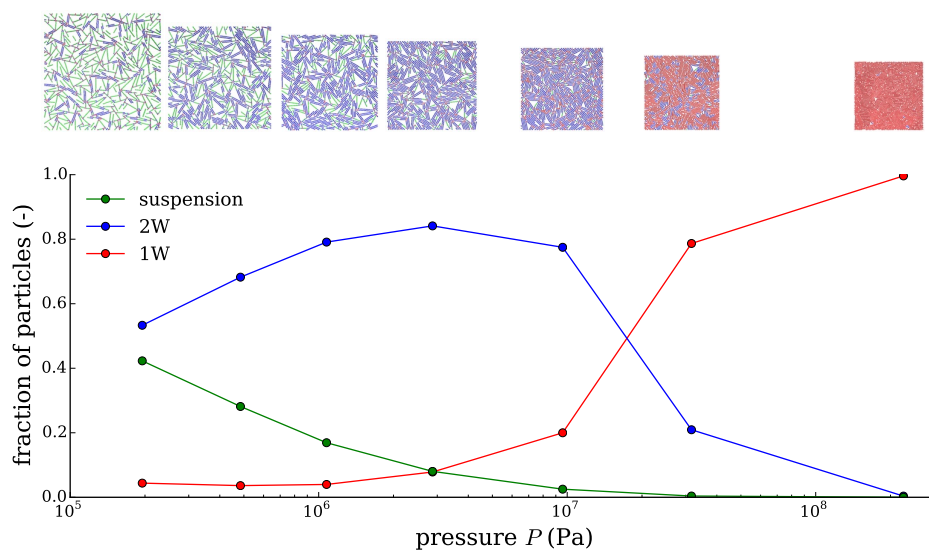


Figure 8: Evolution of the populations of hydration state (1W, 2W, suspension) during the isotropic compression for the meso-structure (a) of Fig. 3. The snapshots illustrate the spacial distribution of the hydration state within the meso-structure, by coloring the the particle depending on their hydration state (green for suspension, blue for 2W, and red for 1W).

transition can be triggered by compression (suspension to 2W, and 2W to 1W), it is interesting to see that the transitions are distributed over a wide range of pressures (more than one order of magnitude) which suggests a major role of heterogeneity. As a consequence, while molecular scale investigation predict 2W-1W transitions above 100 MPa, we find here that already a significant proportion of 1W have appeared at pressures one order of magnitude smaller (20% of 1W at 10 MPa). This results highlight the importance of micro- and meso-structures in the fundamental understanding of clay mechanics.

### 3.2 Drying/humidification

The usual way to induce de-hydration and re-hydration is by applying osmotic loadings. The most obvious osmotic loading is the change of relative humidity in unjacketed conditions, for which 2W-1W transition is expected around 65% humidity. As explained in the methods, a simple way to simulate an osmotic swelling for the meso-scale model is to vary the reference force  $F_0$ : a low value of  $F_0$  favors the 1W state (de-hydration), whereas a high value favors the 2W state (re-hydration). The reference case (Na-Mnt at 100% RH and no confining pressure) corresponds to  $F_0 = 2.5F_0^{eq}$ , which is favorable to the 2W state. A drying is simulated by decreasing the reference force to  $F_0 = -1.0F_0^{eq}$ , which corresponds to an energetically symmetric situation in which 1W is favored (Fig. 5 left). Changes in  $F_0$  can be interpreted roughly as the equivalent of changes in capillary pressure induced by the evolution of relative humidity. A less well-known osmotic loading is the drained heating/cooling under saturated conditions and constant confining pressure, for which heating is expected to trigger de-hydration and cooling re-hydration, at temperatures that depend on the applied confining pressure. In that context, changes in  $F_0$  would correspond to the decrease in disjoining pressure peaks induced by heating. Interestingly, heating tests have shown that the consolidation history controls the magnitude of thermal compaction: normally consolidated clays (i.e., current confining pressure is the maximum of the loading history) exhibit much larger compaction than over-consolidated clays (i.e., current confining pressure smaller than the maximum of the loading history) [3]. The meso-scale model does capture this phenomenon: a normally

consolidated systems exhibits a much larger irreversible contraction than an over-consolidated system when submitted to a  $F_0$ -driven osmotic loading (Fig. 5). How loading history can be related to hydration remains poorly understood, and the meso-scale model offers here a detailed picture of the origin of this phenomenon at the scale of the clay matrix. We display in Fig. 9 the evolution of the proportions of hydration state as a function of the reduced volume, along with a series of snapshots where particles are colored depending on their respective hydration state. For both the normally consolidated and the over-consolidated systems, most of the irreversible contraction corresponds to the change from 2W to 1W state. However, the normally consolidated system experiences much more 2W-1W transitions, than the over-consolidated system (80% of 2W converted vs. 42%). Snapshots of the over-consolidated system clearly highlight that hydration states are homogeneous within stacks of clay layers but inhomogeneous between stacks, suggesting that only the most compressed stacks have changed from 2W to 1W. In contrast, snapshots of the normally consolidated system show a quite homogeneous hydration distribution where almost all stacks have changed from 2W to 1W. Because of their respective loading histories, the two systems are expected to have quite different stress distributions within the meso-structures, which are likely to be responsible for the strong difference in osmotic behavior. This result shows that a description of stress heterogeneity within the clay matrix is necessary to capture the thermal compaction phenomenon, and more generally the response to osmotic loadings.

## 4 Conclusion

In this paper, we use a newly developed granular model of swelling clay matrix to investigate the evolution of the sub-micrometric meso-structure during THM loadings. The model is a pure bottom-up approach coarse grained from molecular simulation results, which is quantitatively consistent with the usual THM behavior of clay matrix (e.g., consolidation curve, swelling...). The characteristics of the meso-structure investigated are the local anisotropy (nematic order parameter), the flexibility of clay layers, and the proportion of the different hydration states. The following conclusion can be drawn from this study:

- At confining pressures approaching 10 MPa, the consolidation curve and the local anisotropy characterizing the degree of stacking appear very similar irrespective of the initial meso-structure before consolidation. This suggests that the clay matrix loses memory of its initial meso-structure at high pressures.
- While layer stretching appears negligible in the mechanical response, layer bending becomes significant at confining pressures exceeding 1 MPa, and it represents more than 10% of the total interaction energy at 10 MPa. The approximation of rigid clay layers is therefore valid only at pressures below 1 MPa.
- Hydration transition induced by compression is progressive in the meso-structure because of stress heterogeneity. Significant fractions of hydration transitions are triggered at confining pressures one order of smaller than the theoretical limit corresponding to perfectly parallel clay layers.
- The consolidation history strongly affects the hydration transition upon osmotic loading, which explains why thermal compaction is much more important for normally consolidated clays than for over-consolidated clays.

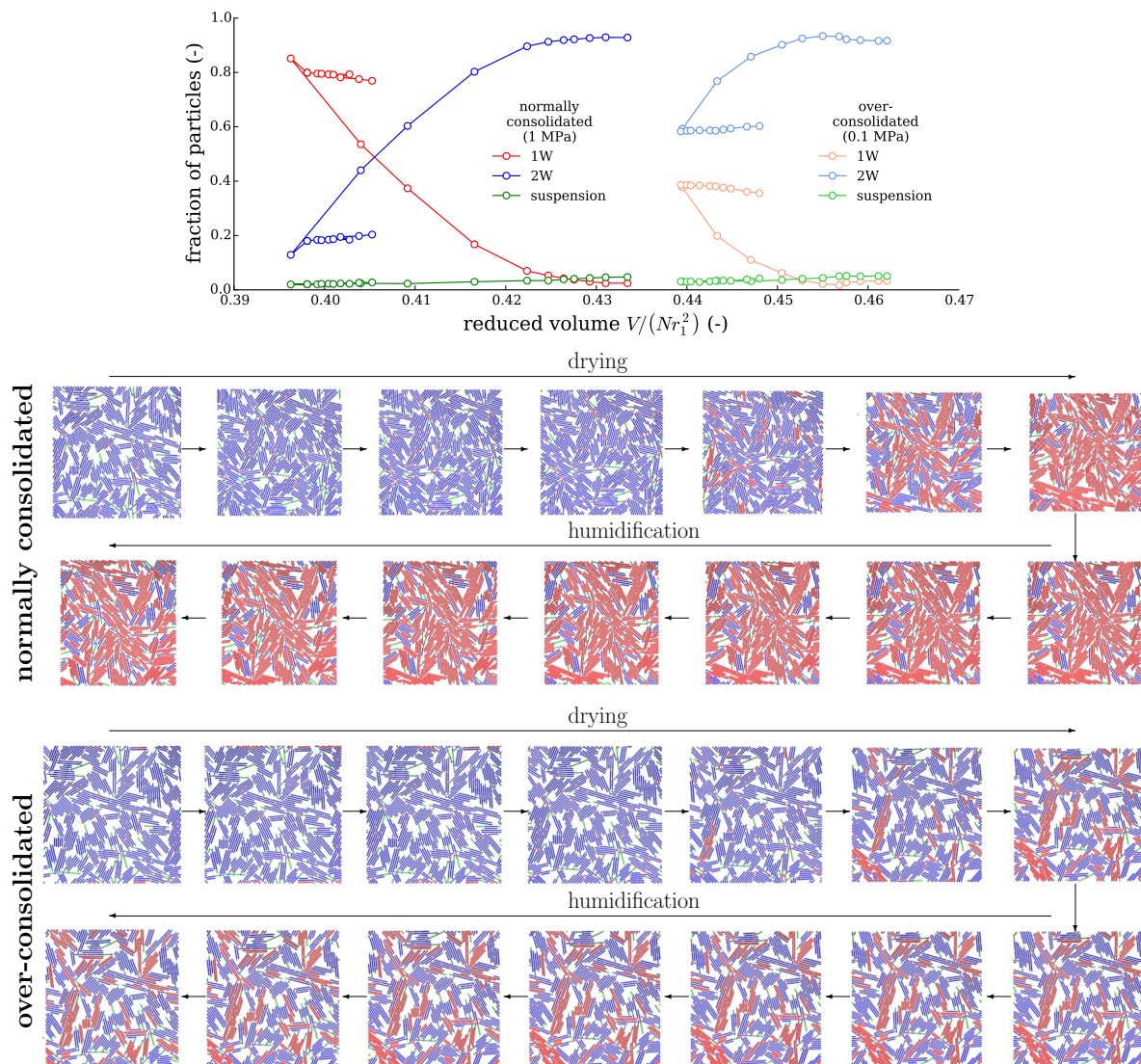


Figure 9: Evolution of the proportion of hydration states during osmotic loading, simulated by varying the reference force  $F_0$ . The proportion of the different hydration states is represented as a function of the induced change in volume, which shows that most of the irreversible contraction is due to the 2W-1W hydration transition. The two consolidation histories considered (normally consolidated, and over-consolidated) exhibit very different compaction, showing the critical importance of the loading history. Snapshot of the meso-structures illustrate the spatial distribution of the hydration states, and its evolution during the osmotic loading.

## References

- [1] F. Asadi, H.-X. Zhu, M. Vandamme, J.-N. Roux, and L. Brochard. A meso-scale model of clay matrix: Role of hydration transitions in the geomechanical behavior. *submitted*, 2022.
- [2] Laurent Brochard. Swelling of Montmorillonite from Molecular Simulations: Hydration Diagram and Confined Water Properties. *The Journal of Physical Chemistry C*, 125(28):15527–15543, jul 2021.
- [3] Laurent Brochard, Túlio Honório, Matthieu Vandamme, Michel Bornert, and Michael Peigney. Nanoscale origin of the thermo-mechanical behavior of clays. *Acta Geotechnica*, 12(6):1261–1279, dec 2017.
- [4] Benoît Carrier. *Influence of water on the short-term and long-term mechanical properties of swelling clays: experiments on self-supporting films and molecular simulations*. PhD thesis, Université Paris Est, 2013.
- [5] Tulio Honorio, Laurent Brochard, Matthieu Vandamme, and Arthur Lebée. Flexibility of nanolayers and stacks: implications in the nanostructuration of clays. *Soft Matter*, 14(36):7354–7367, 2018.
- [6] D. Tessier. Behaviour and Microstructure of Clay Minerals. In M.F. De Boodt, M.H.B. Hayes, A. Herbillon, E.B.A. De Strooper, and J.J. Tuck, editors, *Soil Colloids and Their Associations in Aggregates*, NATO ASI Series (Series B: Physics), pages 387–415. Springer, Boston, MA, 1990.